

# Study of some physical properties of organic dye thin films and photovoltaic application

#### Thesis Presented by

#### Lamiaa Mahmoud Diaa El-Deen Mohamed

For the degree Master of Teacher's Preparation in Science (Solid State Physics)

#### Supervised by

# Dr. Attia Abd El-Motteleb Attia

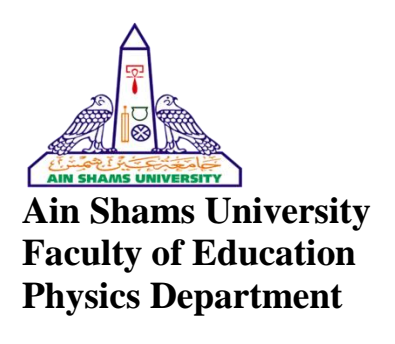
Assistance Prof. of Solid State physics Physics Dept., Faculty of Education Ain Shams University

# Dr. Enas Abd EL-Fattah El-shazly

Assistance Prof. of Solid State physics Physics Dept., Faculty of Education Ain Shams University

# Dr. Amal Mohammed Abd El-barry

Assistance Prof. of Solid State physics Physics Dept., Faculty of Education Ain Shams University



Researcher name: Lamiaa Mahmoud Diaa El-Deen Mohamed

**Title of The Thesis**: Study of some physical properties of organic dye thin films and photovoltaic application

**Submitted to:** Physics Department, Faculty of Education, Ain Shams University

# **Supervisors:**

1-Dr. Attia Abd El-Motteleb Attia

2- Dr. Enas Abd EL-Fattah El-shazly

3- Dr. Amal Mohammed Abd El-barry

## **Approval sheet**

**Title**: Study of some physical properties of organic dye thin films and photovoltaic application

Candidate: Lamiaa Mahmoud Diaa El-Deen Mohamed

**Degree:** Master of Teacher's Preparation in Science (Solid State Physics)

#### **Board of Advisors**

# Approved by:

#### 1-Dr. Attia Abd El-Motteleb Attia

Assistance Prof. of Solid State physics Physics Dept., Faculty of Education Ain Shams University

## 2- Dr. Enas Abd EL-Fattah El-shazly

Assistance Prof. of Solid State physics Physics Dept., Faculty of Education Ain Shams University

# 3- Dr. Amal Mohammed Abd El-barry

Assistance Prof. of Solid State physics Physics Dept., Faculty of Education Ain Shams University

Date of Presentation: / /2018

# **Post graduate studies:**

Stamp: / /2019 Date of Approval: / /2019

Approval of Faculty Council: / / 2019

## **Acknowledgement**

First of all, I would like to thank ALLAH who gave me the strength for accomplishing this thesis. I praise him as much as the heavens and earth and what are in between and behind.

First, I would like to express my gratitude to Prof. Dr. M. M. El-Nahass, the professor of solid-state physics, faculty of Education, Ainshams University. I thank him from my deep heart for his fatherhood, motivation, continuous supervision, useful discussion and insightful advice. Working in his laboratory was one of the most challenging and exciting experience of my life. Many thanks for physics group working with Prof. Dr. M. M. El-Nahass.

Deepest gratitude to Dr. Attia Abd El-Motteleb Attia for his advice, valuable help and Encouragement during this Study. I thank him from my deep heart for his fatherhood, motivation, continuous supervision, useful discussion and insightful advice.

The Author wishes to thank Dr. Enas Abd EL-Fattah El-shazly for her valuable help and Encouragement during this Study.

Thanks goes also to Dr. Aml Mohamed Abd El-barri for her help and advice through the period of this research work.

Many appreciations are for the head of physics department and all the staff members of thin film laboratory, faculty of Education, Ain shams university, for their friendly cooperation and encouragement.

I would like to record my gratitude to my family, my mother, my sister and my husband for their love, patience and support through my life and studies. Finally I am devoting this thesis to the memory of my father, Prof. Dr. Mahmoud Diaa El-Deen Mohamed.



# **Contents**

Page
List of Tables
List of Figuresii
Abstractvi Summeryviiii
Introductionx
Chanten I
<u>Chapter I</u> <u>Theoretical Background and Literature Review</u>
1.1 Theoretical Background
1.1.1 Organic Semiconductors
1.1.1.1 Basic Properties of Organic Semiconductors1
1.1.1.2 Deposition Techniques
1.1.1.3 Semiconducting Properties of Organic Materials2
1.1.1.4 Electronic structure of organic semi conductors4
1.1.1.5 Charge Carrier Transport
1.1.2 Back ground of Porphyrins
1.1.3 Optical properties10
1.1.3.1 Absorption and optical properties of organic material11
1.1.3.2 Four-Orbital Model12
1.1.3.3 Optical properties of semi conductors13
1.1.3.4 Absorption at fundamental absorption edge14
1.1.3.5 Absorption process (direct and indirect transitions)16
1.1.3.6 Measurement of Light Absorption
1.1.3.7 Absorption Intensity; Oscillator Strength18
1.1.3.8 Dispersion in semiconductors
1.1.3.9 The volume and surface energy loss functions22

1.1.3.10 The optical conductivity	22
1.1.4 Organic photovoltaic	22
1.1.5 Basic processes in organic solar cells	24
1.1.6 The conduction mechanism of p-n junction	25
1.1.7 Photovoltaic characteristics of a Solar cell	29
1.1.8 Photovoltaic solar cell parameters	32
1.2 Literature Review	33
1.2.1 Introduction	33
1.2.2 Structural properties of porphyrins	33
1.2.3 Optical properties of porphyrins	36
1.2.4 Photovoltaic Properties of porphyrins	42
Chapter II  Experimental techniques	
Experimental techniques 2.1 Material Investigation	44
2.2 Thin films preparation	45
2.2 Thin films preparation      2.2.1 Thermal Evaporation Technique	
	45
2.2.1 Thermal Evaporation Technique	45
2.2.1 Thermal Evaporation Technique  2.3 Methods for film thickness measurement	45 46 46
2.2.1 Thermal Evaporation Technique  2.3 Methods for film thickness measurement	45 46 46
2.2.1 Thermal Evaporation Technique  2.3 Methods for film thickness measurement	45 46 46 47
2.2.1 Thermal Evaporation Technique	45 46 46 47 49
2.2.1 Thermal Evaporation Technique	45 46 46 47 49 49
2.2.1 Thermal Evaporation Technique	45464647495051
2.2.1 Thermal Evaporation Technique	45464647495051

2	2.5.2 Determination of the optical constants54
2.6.0	Cyclic voltammetry54
2.7 A	Au/MnTPPCl/p-Si/Al Hetero junction56
2	2.7.1 Devices preparation56
2	2.7.2 Current – Voltage (I-V) measurement57
,	2.7.3 Capacitance -Voltage (C-V) measurement58
	<u>Chapter III</u> <u>Structural Properties of MnTPPCl Thin films</u>
3.1 X	X-Ray Diffraction Patterns59
3	3.1.1 X-ray diffraction of MnTPPCl in powder form59
3	3.1.2 X-ray diffraction of as deposited MnTPPCl thin films62
3	3.1.3 Effect of heat treatment on the structural characterization of MnTPPCl thin films
	Scanning electron microscope (SEM) investigation for as-deposited and annealed films
	Chapter IV Optical Properties of MnTPPCl Thin films
4.1	Effect of thickness film on the optical properties of MnTPPCl thin films
4	4.1.1 Transmission and reflection spectra
	4.1.2 Determination of the refractive index (n) and absorption ndex(k)
4	4.1.3 Absorption Characterizations70
4	1.1.4 Dielectric Characterization71
4	4.1.5 Volume energy loss and Surface energy loss of thin films72
4	4.1.6 Optical Conductivity73
4	4.1.7 Molar Extinction Coefficient75

4.1.8 HOMO-LUMO Gap Determination76		
4.1.9 Dispersion parameters		
4.1.10 Non Linear optical characteristics of MnTPPCl films80		
4.2 Effects of Annealing Temperatures on Optical Properties of MnTPPCl Thin Films		
4.2.1 Transmittance and reflection spectra83		
4.2.2 Determination of the refractive index (n) and absorption index (k)		
4.2.4 Dielectric Characterization		
4.2.5 Volume energy loss and surface energy loss of thin films89		
4.2.6 Optical Conductivity90		
4.2.7 Determination of HOMO-LUMO gap93		
4.2.8 Dispersion Parameters95		
4.2.9 Non linear optical characteristics of MnTPPCl thin films97		
<u>Chapter V</u> <u>MnTPPCl /p-Si Organic –Inorganic Photovoltaic cells</u>		
5.1 Introduction		
5.2 Dark current-Voltage characteristics98		
5.3 Rectification Ratio (RR)99		
5.4 Conduction Mechanism		
5.5 Series and Shunt Resistances		
5.6 Temperature dependence of IR-V characteristics106		
5.7 Dark Capacitance-Voltage characteristics		
5.8 Photovoltaic Properties 110		

Conclusion	112
References	115
Arabic Summery	

# **List of Tables**

I	Page
Table 3-1: Crystal data for the powder of meso-tetraphenylporphyrin.manganese	
(III)chloride	59
Table 3-2: Indexing of the diffraction data of MnTPPCl in the powder form	61
Table 3-3: Structural parameters for powder and annealed MnTPPCl thin films	63
<b>Table 3-4:</b> IR Spectral data for the powder, as deposited thin film and annealed thin film of MnTPPCl	67
<b>Table 4.1:</b> The energy in eV of peaks obtained from k, ε <sub>2</sub> , tanδ, VELF, SELF and σ1spectra of MnTPPCl thin films.	74
<b>Table 4.2:</b> The energy in eV of peaks obtained from n, $\varepsilon_1$ and $\sigma_2$ spectra of	
MnTPPCl thin films.	75
<b>Table 4.3:</b> Calculated values of the oscillator strength, f, and the electric dipole,	
q <sup>2</sup> , for the as deposited MnTPPCl thin films at different bands	<b>76</b>
Table 4.4: dispersion parameters of as-deposited MnTPPCl thin films compared	
with other related organic films.	80
<b>Table 4.5:</b> The energy in eV of peaks obtained from k, $\varepsilon_2$ , tan $\delta$ , VELF, SELF and $\sigma$ 1 spectra of as-deposited and annealed MnTPPCl thin films.	92
<b>Table 4.6:</b> The energy in eV of peaks obtained from n, $\varepsilon_1$ and $\sigma_2$ spectra of as-	
deposited and annealed MnTPPCl thin films.	92
Table 4-7 The values of optical band gap for the as-deposited and annealed	
MnTPPCl thin films	94
Table 4.8: Dispersion parameters of the as deposited and annealed MnTPPCl	
Thin films	96
Table 4.9: Energy gap Eg, maximum values of the non linear absorption	
coefficient $\beta_{max}$ , values of the energy corresponding to $\beta_{max}$ ,	
$E_{\beta}$ =max, ratio of $E_{\beta}$ /=max for as-deposited and annealed MnTPPCl	
thin films.	97
Table 5.1: The estimated values of RR, I <sub>0</sub> 1, I <sub>0</sub> 2, n <sub>1</sub> and n <sub>2</sub> for Au/MnTPPCl/p-Si/	
Al heterojunctions at different temperatures.	102
<b>Table 5.2:</b> The values of $E_t$ at different voltage	104

# **List of Figures**

		Page
Figure 1.1:	Different hybridizations for the carbon atom where (a) sp <sup>3</sup> hybridization (b) sp <sup>2</sup> hybridization (c) sp hybridization.	3
Figure 1.2:	Schematic representation of splitting of two 2p orbitals	
	into a bonding molecular $\pi$ -orbital and anti- bonding $\pi^*$ -	
	orbital. Increasing the number of carbon atoms, leads to	4
	more degeneration and the formation of quasi-continuous	
	bands of occupied and un occupied states.	
Figure 1.3:	The electronic energy levels and transitions.	6
Figure 1.4:	Energy levels of an isolated molecule (left) and a molecular	
	crystal(right): Ig and Ag denote the ionization potential and	
	electron affinity in the gasphase, Ic and Ac the respective	
	quantities in the crystal. Due to the polarization energies Ph	_
	and Pe charged states are stabilized in the crystal. Eg is the	7
	Single-particle gap being relevant for charge carrier generation,	
	whereas Eopt denotes the optical gap measured in absorption	
	and luminescence. Their difference is the so-called exciton	
T 1 F.	binding energy.	
Figure 1.5:	Energy levels of an isolated molecule (left), a molecular crystal	7
Elaura 1.6.	(middle) and an amorphous solid (right).	0
Figure 1.6:	The basic structure of the porphyrin macro cycle	9
Figure 1.7:	Schematic diagram showing reflection, propagation and	11
Figure 1 Q.	transmission of the incident light on an optical medium	
Figure 1.8:	Energy diagram and electronic transition in (a) a molecule, and (b) a bulk solid.	12
Figure 1.9:	Porphyrin HOMOs and LUMOs. (A) Representation of the	
rigure 1.7.	four Gouterman orbitals in porphyrins. (B) Drawing of the	
	energy levels of the four Gouterman orbitals up on Symmetry	13
	lowering from D4h to C2V. The set of eg orbitals gives rise to	
	Q and B bands.	
Figure1.10:	Hypothetical absorption spectrum for typical semiconductor as	1.4
G	a function of photon energy.	14
Figure 1.11:	Typical spectral dependence of the optical absorption	15
	coefficient α in amorphous semiconductors	13
<b>Figure 1.12:</b>	Type of electronic transition (a) direct transition and (b)	17
	indirect transitions.	1.7
<b>Figure 1.13:</b>	(a) cathode to anode potential distribution in a vacuum diode (i)	
	in the absence of electron flow, (ii) thermionic emission limited	
	current flow (iii) space charge limited flow of electrons. (b)	
	Potential distribution across a metal semiconductor contact,	
	where the metal contact is maintained at zero-bias, (i) under	_
	applied forward bias, and (ii) reverse bias.	27

Figure 1.14:	The equivalent circuit diagram for an ideal solar cell	30
<b>Figure 1.15</b> :	Typical I-V characteristics for a solar cell in the dark and under	32
<b></b>	illumination	
Figure 1.16:	(TGA) curve for powder of MnTPPCl.	42
Figure 2.1:	Molecular structure of MnTPPCl	44
Figure 2.2:	Schematic diagram of vacuum and evaporating system (Model E306A, Edwards Co England).	45
Figure 2.3:	(a) Schematic diagram of the interferometer; (b) schematic diagram showing the optical set-up for film thickness measurements; where S is Thallium lamp, A is a circular aperture, B is a slit, C is a collomating lens, D is monochromatic filter and E is a polarization microscope; (c) Fizeau fringes.	48
Figure 2.4: Figure 2.5:	Geometric arrangement of X-ray diffractometer. Schematic of a Scanning electron microscope.	50 50
Figure 2.6:	The Scanning electron microscope model Quanta 250 (Field emission gun)	51
Figure 2.7:	Schematic diagram of the infrared spectrophotometer	52
Figure 2.8:	Schematic diagram showing the spectrophotometer	52
Figure 2.9:	Measurement of film transmission where the reference is clean substrate	53
<b>Figure 2.10:</b>	Measurement of film reflectance where the reference (Almirror) is in front of the sample	54
<b>Figure 2.11:</b>	Simple diagram of cyclic voltammetry experiment	55
<b>Figure 2.12:</b>	Schematic diagram of the oxidation and reduction of an organic molecule.	56
<b>Figure 2.13:</b>	Schematic device structure of Au/MnTPPCl/p-Si/Al heterojunctions.	56
<b>Figure 2.14:</b>	(a) circuit for measuring the I-V Characteristics using CRO (b) Circuit for measuring the I-V Characteristics point by point in dark and under illumination.	57
<b>Figure 2.15:</b>	simplified block diagram of model 4108C-V meter.	58
Figure 3.1:	X-ray diffraction pattern (XRD) for MnTPPCl: (a) powder (b)	
	as-deposited film (c) film annealed at 423 K (d) film annealed at 473 K (e) film annealed at 523 K	60
Figure 3.2:	SEM image for MnTPPCl thin films (a) as deposited, (b) annealed at 473k and (c) annealed at 523 k; the inset figure for	64
Figure 2.2.	a magnified image of the pyramidal shape of a particle.  Infrared spectra of MnTPPCl: (a) powder form; (b) thin film as	04
Figure 3.3:	deposited 253 nm; (c) thin film annealed at 423 K; (d) thin film annealed at 473 K; (e) thin film annealed at 523 K for 2 h.	66
Figure 4.1:	The transmittance $T(\lambda)$ , and the reflectance $R(\lambda)$ for the as deposited MnTPPCl thin films with different thickness.	68
Figure 4.2:	The spectral dependence of the mean values of real, n, and	
8	imaginary, k, parts of refractive index for MnTPPCl thin films.	69
Figure 4.3:	Photon energy dependence of the optical absorption coefficient, $\alpha$ (hv), of MnTPPC1 thin films.	71
Figure 4.4:	Photon energy dependence of both $(\epsilon_1, \epsilon_2)$ of MnTPPCl thin films; the inset for $tan(\delta)$ vs. hv.	72

Figure 4.5:	Photon energy dependence of VELF and SELF of MnTPPCl thin films	73
Figure 4.6:	Photon energy dependence of $\sigma_1$ and $\sigma_2$ of MnTPPCl thin films	74
Figure 4.7:	Shows the plot of $\varepsilon$ molar as a function of the wave number ( $\upsilon$ )	76
	for as-deposited MnTPPCl thin films.	70
Figure 4.8:	Plot of $(\alpha h \nu)^2$ vs $(h \nu)$ of MnTPPCl thin films, the inset figure for	78
	the onset transition(1.92 eV)	70
Figure 4.9:	Cyclic voltammetry (CV) data of MnTPPCl	<b>78</b>
<b>Figure 4.10:</b>	Plot of $(n^2-1)-1$ vs. $(hv)^2$ of MnTPPCl thin films.	<b>79</b>
<b>Figure 4.11:</b>	Plot of $n^2$ vs $\lambda^2$ of as-deposited MnTPPCl thin films.	80
<b>Figure 4.12:</b>	Non-linear absorption coefficient $\beta_c$ of MnTPPCl thin films as	81
	a function of incident photon energy (hv).	01
<b>Figure 4.13:</b>	The transmittance, T ( $\lambda$ ) for the as deposited and annealed	83
	MnTPPCl thin films at different temperature.	00
<b>Figure 4.14:</b>	The reflectance, R ( $\lambda$ ) for the as deposited and annealed	84
	MnTPPCl thin films at different temperature.	0.
<b>Figure 4.15:</b>	The spectral dependence of refractive index, n, for as-deposited	85
	and the annealed MnTPPCl thin films.	
Figure 4.16:	Extinction coefficient, k for as-deposited and annealed films as	85
T' 4.15	a function of wave length	
<b>Figure 4.17:</b>	Spectral behavior of absorption coefficient, $\alpha$ , for the as-	86
E: 4 10.	deposited and annealed MnTPPCl thin films.	
Figure 4.18:	Photon energy dependence of $\varepsilon_1$ for the as-deposited and	87
E 4 10.	annealed MnTPPCl thin films.	
<b>Figure 4.19:</b>	Photon energy dependence of $\varepsilon_2$ for the as-deposited and annealed MnTPPCl thin films.	88
Figure 4.20:	The variation of the loss factor with photon energy for the as-	
Figure 4.20.	deposited and annealed MnTPPCl thin films	88
<b>Figure 4.21:</b>	Photon energy dependence of VELF for the as-deposited and	
11gure 4.21.	annealed MnTPPCl thin films.	89
<b>Figure 4.22:</b>	Photon energy dependence of SELF for the as-deposited and	
<b>g</b>	annealed MnTPPCl thin films.	90
<b>Figure 4.23:</b>	Photon energy dependence of $\sigma_1$ for the as-deposited and	
<b>_</b>	annealed MnTPPCl thin films.	90
<b>Figure 4.24:</b>	Photon energy dependence of $\sigma_2$ for the as-deposited and	0.1
8	annealed MnTPPCl thin films.	91
<b>Figure 4.25:</b>	The $(\alpha h \nu)^2$ vs $(h \nu)$ plot for the as-deposited and annealed	0.4
	MnTPPCl thin films	94
<b>Figure 4.26:</b>	Plot of $(n^2-1)^{-1}$ as a function of $(hv)^2$ for as-deposited and	95
	annealed MnTPPCl thin films.	93
<b>Figure 4.27:</b>	Plot of of $n^2$ as a function of $\lambda^2$ for as-deposited and annealed	96
	MnTPPCl thin films.	70
<b>Figure 4.28:</b>	Non linear absorption coefficient $\beta_c$ of as-deposited and	97
	annealed MnTPPCl thin films.	71
Figure 5.1:	I-V characteristics of MnTPPCl/p-Si heterojunctions at	
	different temperature and the voltage dependence of ln I inset	99
	it.	
Figure 5.2:	Semi logarithmic plot of the forward and reverse current of	400
	MnTPPCl/p-Si hetero junction against voltage at room	100
	temperature	

Figure 5.3:	Semi-logarithmic plot of forward bias (I-V) characteristics of Au/MnTPPCl/p-Si/ Al heterojunctions at different temperature.	101
Figure 5.4:	a plot of $\ln \frac{I_{\circ}}{T^2} \text{ vs } \frac{1000}{T}$ for Au/MnTPPCl/p-Si/ Al	103
	heterojunctions	
Figure 5.5:	Variation of logI with logV at higher forward voltage bias for MnTPPCl/p-Si.	103
Figure 5.6:	Shows the temperature dependence of ln (I) at 0.7, 1, 1.5 volt.	104
Figure 5.7:	Variation of ln (I) vs. V at room temperature in forward bias. The inset shows plot of $\delta V$ against I.	105
Figure 5.8:	Plot of Rj vs. V for MnTPPCl/p-Si a) at 293K, b) at 313 K, c) at 333K, d) at 353K and e) at 373K.	106
Figure 5.9:	Temperature dependence of ln (IR) for MnTPPCl/p-Si hetero junction	107
Figure 5.10:	Reverse bias I-V for MnTPPCl/p-Si hetero junction at different temperatures showing a linear dependence of ln (IR) on V <sup>1/2</sup> .	108
Figure 5.11:	plot of $\frac{1}{c^2}$ against voltage of MnTPPCl/p-Si heterojunctions at	110
E:	room temperature	
Figure 5.12:	A plot of I-V characteristics of heterojunctions Au/MnTPPCl/p-Si/Al under illumination conditions.	111